Enabling the injection of hydrogen in high-pressure gas grids: investigation of the impact on materials and equipment

Javier Sánchez-Laínez[1*], Alberto Cerezo[2], Mª Dolores Storch de Gracia[2,3], Jorge Aragón[4], Ekain Fernandez[4], Virginia Madina[4], Vanesa Gil,[1,5*]

[1]*Foundation for the Development of New Hydrogen Technologies in Aragon, Parque Tecnológico Walqa Ctra. N-330A, km. 566, 22197, Cuarte, Huesca, Spain*
[2]*Redexis, C/ Mahonia 2, 28043 Madrid, Spain*
[3]*Universidad Politécnica de Madrid, 28040 Madrid, Spain*
[4] *TECNALIA, Basque Research and Technology Alliance (BRTA), Mikeletegi Pasealekua 2, 20009 Donostia-San Sebastián, Spain.*
[5]*ARAID Foundation, Avda. de Ranillas 1-D, 50018 Zaragoza, Spain*

(*) vgil@hidrogenoaragon.org

ABSTRACT

Green hydrogen is a renewable gas that can help to reach the goal of decarbonizing the energy sector. The use of the natural gas grid for seasonal storage and transport of hydrogen needs previous assessment of its tolerance, ensuring safe and viable operation. In this work, the tolerance of the most typical material pipelines and key elements of high-pressure gas grids to the transport of 20 mol % hydrogen blends at 80 barg has been investigated at pilot scale. For this, the experimental campaign carried out at a testing platform replicating a high-pressure gas grid lasted 3000 hours. The tightness of different kind of valves led to hydrogen losses below 1 $Nml \cdot h^{-1}$. No embrittlement or other kind of damage was found on these valves or the different parts of the equipment (regulator, flowmeter) tested. C-ring, 4pb and CT-WOL specimens have been prepared from carbon steel pipes (API5L Gr X42 to X70), showing no damage after exposure to hydrogen. H_2/CH_4 deblending has also been successfully achieved using Pd-based membrane technology, obtaining a high-purity separated streams.

KEYWORDS: Hydrogen injection, H2/NG blend, retrofitting, high-pressure gas grid, transmission

1. INTRODUCTION

Green hydrogen is one of the most promising renewable gases that can lead to aim the decarbonization of the energy sector. Renewable hydrogen, also known as green hydrogen, is an energy carrier that has to be produced using electric power in water electrolysis processes.[1] Wind, solar, and other renewable sources can produce large amounts of energy. However, the energy produced by these sources is intermittent, and can therefore only be stored for long periods of time if hydrogen is used as energy carrier. Afterwards, hydrogen can be back converted into electricity with fuel cell devices, solving the problem of the low storage capacity of the electrical grid. The use of hydrogen as fuel is also possible via direct burning in compatible engines, boilers, etc. To limit the global warming to 1.5 °C, as stated in the Paris Agreement, implies net zero CO_2 emissions by 2050. The REPowerEU Plan sets out that an additional 15 million tons (Mtons) of renewable hydrogen – on top of the 5.6 Mtons already planned under the Fit for 55 initiative. This numbers can replace approximately 27 bcm of imported Russian gas by 2030. To reach this goal, energy savings, diversification of energy supply and

accelerated deployment of renewable energies are essential to decarbonize critical sectors.

For the successful commercialization of hydrogen, a safe and reliable delivery infrastructure is required. Compressed gaseous hydrogen can be transported by pipelines, railroads, tanker trucks or tanker ship. The chosen method is a matter of cost, based on the distance of transportation and the amount of gas to transport.[2] Retrofitting existing natural gas pipelines is potentially the most economical way to establish an infrastructure to transport hydrogen across continental distances without developing a dedicated infrastructure.[3] At the same time, it can also serve as a means of transporting large volumes of green hydrogen (produced at low cost in areas with a high percentage of renewables) to final users. However, it is necessary to assess compatibility of the natural gas infrastructure towards hydrogen to ensure a safe and efficient use of the grid for the delivery of this new gas. [4]

There are two options for transporting hydrogen via natural gas pipelines, a) as a blend and b) 100 mol % hydrogen, and both need of injection facilities in which hydrogen is added to the gas grid. The former consists in adding a certain amount of hydrogen into a gas pipeline that is already transporting natural gas, obtaining a Hydrogen/Natural Gas (H_2/NG) blend with a defined percentage of hydrogen in it. The latter implies replacing natural gas completely by hydrogen as the new fuel to transport. The transport as a blend is the best approach when the production of hydrogen is not sufficient enough to replace the energy content in natural gas and the end users downstream the injection point can allocate certain amounts of hydrogen in the fuel gas.[5] Preliminary studies from ENTSOG have shown that the transport of a mixture of natural gas and hydrogen is possible without pipeline modification as long as the mass fraction of hydrogen remains sufficiently low. According to one of their reports, blending percentages up to 2 vol. % H_2 into the natural gas system are already possible without any additional mitigation efforts.[6] Higher concentrations may need for adaptations in the infrastructure, regardless the pressure level in the grid. This fact is due to the different physical and chemical properties of hydrogen in comparison with those of natural gas. Owing to this fact, blending hydrogen with natural gas may have an impact on 1) safety issues, because the potential leakage rate of hydrogen is much larger than that of natural gas through the same sized leak, 2) pipeline integrity, due to possible hydrogen embrittlement mechanism, 3) gas quality, because the combustion properties change when hydrogen is added to natural gas, having a direct impact on end uses.[7] Some plans for repurposing grid for 100 mol% hydrogen transport are also under development. The hydrogen European Backbone[8] updated report states that by 2030, five pan-European hydrogen supply and import corridors could emerge, connecting industrial clusters, ports, and hydrogen valleys to regions of abundant hydrogen supply. The hydrogen infrastructure will grow to around 53,000 km length by 2040, mostly based on repurposed existing natural gas infrastructure.

Most studies about retrofitting the natural gas grid consider just the impact of hydrogen in end-uses, specifically combustion issues, checking for instance the effect that hydrogen has on the performance of burners and the combustion process itself (power, efficiency, emissions, etc.).[9-11] However, a deeper research on the impact of hydrogen in the materials composing all the components and equipment in the grid is essential to check

the readiness of the gas infrastructure towards the new fuel and perform necessary adaptations. This study is even more critical for the transmission network, being the part of the gas grid composed of wide-diameter pipelines that connect the entry point of natural gas to the system to main consumer service areas over long distances. It has the particularity of working at high operating pressure, making the possible damage of hydrogen more acute. In compression and pressure-reduction stations, hydrogen embrittlement issues and gas leakages are key aspects to be considered when analyzing the suitability of the natural gas grid for hydrogen transport.[5]

Hydrogen embrittlement is a process in which the tensile ductility of a material working on hydrogen environment and in the presence of stress concentration, is significantly reduced because of the introduction of hydrogen atoms in its lattice. Additionally, the fracture toughness and fatigue strength of this material decreases.[12-15] The severity of these manifestations of hydrogen embrittlement depends on mechanical, environmental and material variables. The pipelines in high-pressure grids are mainly based on carbon steels, which can be susceptible to hydrogen embrittlement. The risk embrittlement is highly dependent on the steel quality, especially of the microstructure of the steel[16] but also on the conditions to which the material has been exposed. The impact of hydrogen embrittlement on carbon steels with qualities up to API 5L X80 has been studied in the literature to identify the relationship between hydrogen concentration and failure loading with conclusions highly dependent on the testing conditions.[17, 18] Sometimes the results obtained have been unexpected or even controversial. Slifka et. al.[19] performed fatigue crack growth rate tests in hydrogen at 5.5 and 34 MPa with X52 and X70 steels from new and vintage pipes. The vintage X52 material showed more sensitivity to pressure than the other three steels, contrary to the logic expected. Another study states that the propagation of fatigue cracks in X52 steels is faster in presence of hydrogen than in natural gas, which can lead to 20% reduction of safety and security factors when using these pipelines for hydrogen service.[20] It is therefore necessary further research in relevant environment close to real conditions to assess the real impact of hydrogen in these materials.

Since the natural gas grid goal is delivering fuel to end-users, it may be necessary to develop separation technologies when blending scenarios are present, so that those end users that cannot allocate relevant contents of hydrogen in natural gas can remain connected to the grid, and at the same time, the recovered hydrogen can be used for other purposes. The current separation technology is well developed for high concentrations of H_2 in the blend (pressure–temperature swing adsorption or PTSA stations). However, there is still ground for innovation when the hydrogen level in the admixture is low ($\leq$20-30 mol%), which is the range expected in future blending scenarios. Pressure swing adsorption (PSA) and fractional/cryogenic distillation systems are commercially available. They are generally not cost effective, but they are quite energetically demanding, especially when the hydrogen content in the blend is low.[21] Because of this fact, membrane-based processes are considered to be the most promising technologies for the production on one side of a high-purity hydrogen stream and on the other side of another stream concentrated in natural gas (and with very low hydrogen content) from admixture streams $\leq$20 mol% H_2.[22]

3

This work aims to study the suitability of high-pressure natural gas grids for the transport of H_2/NG blends containing up to 20 mol % of H_2. An experimental platform has been built ad hoc to investigate the effect of the blend on the materials and components under relevant environment. This platform is a pilot testing loop that tries to replicate a transport gas facility, in which commonly used pipes, components and equipment of the natural gas grid have been installed to expose them to hydrogen admixtures at 80 barg pressure. The sensitivity to hydrogen (i.e. hydrogen embrittlement) and gas tightness of the different testing items have been assessed during the experimental campaign. Besides, a separation prototype based on membrane technology has been developed and incorporated into the platform to investigate gas separation tests (hydrogen recovery). The research activities of this work are framed within the HIGGS project "Hydrogen in Gas Grids: A systematic validation approach at various admixtures levels into high-pressure grids" (GA No. 875091), pave the way to decarbonization of the gas grid and its usage, by covering the gaps of knowledge of the impact that high levels of hydrogen could have on the gas infrastructure, its components and its management.

2. EXPERIMENTAL SECTION

2.1. Testing facility: Design of the experimental platform

HIGGS approach is based on implementing a project vision that allows the systematic validation systems and components, typically present in high pressure gas grids. To reach this goal an experimental platform has been built ad hoc for this project. This facility consists in a blending station, a testing platform and a gas separation prototype. A scheme of this setup can be seen in Figure 1.
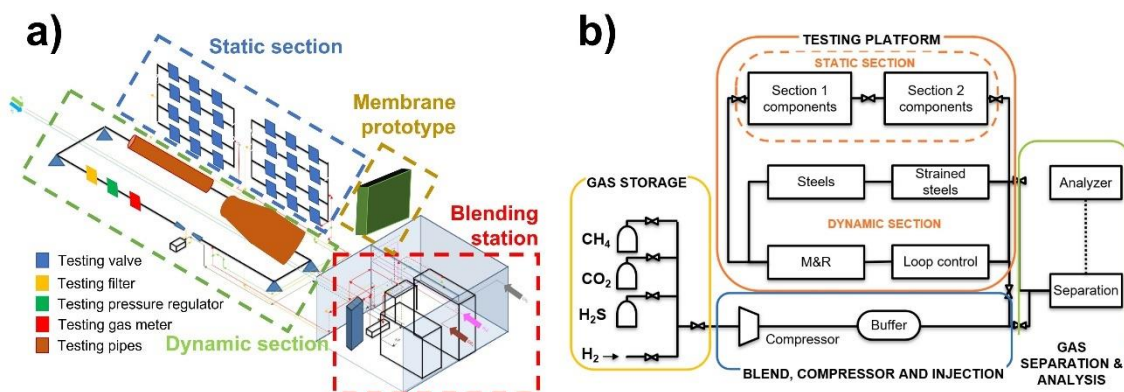

Figure 1. 3-D (a) and 2-D (b) view of a scheme of the testing platform built for this work.

The gas admixture with the target composition is prepared in the blending station, a setup where blends of CH_4, H_2S, CO_2 and CH_4 with a target composition can be prepared and stored at high pressure. CH_4 represents the main component in natural gas (concentration >95 mol %); CO_2 and H_2S; the main impurities that can be found in natural gas, and H_2 is the gas whose impact on materials wants to be studied. This setup can prepare the kind of admixture that would be present in the grid after a hydrogen injection point to which the different testing items are exposed.

In the blending station, pure gas lines at low pressure merge and the resulting blend is compressed and stored (see Figure S1). Each individual gas line of the blending station is fitted with a pressure regulator (Tescom) and a flow controller (Bronkhorst) to add the

right amount of each gas to the blend, and therefore achieve the admixture with the desired hydrogen concentration and ensure the right mixing of the components at the same pressure level (15 bar). All the individual lines merge in one and the admixture flows through a static mixer (Primix) to achieve its complete homogenization. Finally, the admixture is compressed up to 200 bar and stored in a buffer. This buffer feeds the different parts of the testing platform (divided into a dynamic and a static section) and the membrane module to perform the tests that will be explained in the following sections. The selected blend for the tests in this work was 20 mol % H_2 in CH_4 (electrolytic and G20 quality, respectively), avoiding the typical impurities of natural gas to better distinguish the possible damaging effects of hydrogen.

2.2. Gas tightness tests

Hydrogen is a gas with lower density and higher diffusivity than natural gas. Checking the tightness of components of the grid toward hydrogen is therefore necessary to ensure that the levels of fugitive emissions remain within the legal values when the new gas quality is transported. The tightness of several valves towards hydrogen was performed in the static section of the testing platform, which aims to represent a valve node, a typical transmission position in the grid whose goal is sectioning and deriving the gas in the grid. Ball, plug, butterfly and needle valves have been selected as the most representative valves in the grid according to a previous study conducted in HIGGS project[23] and they have been installed using flanged and screw couplings. Detailed information about the testing valves can be seen in Table 1.

Table 1. List of components (valves) and equipment tested in the experimental facility.

Element	Manufacturer	Model	Connection (size and technical standard)	Section
Ball Valve	ALFA VALVOLE	ALFA-606/FB Split Body	F	Static
Lug-type butterfly Valve	DIDTEK	LUG – ZERO LEAKAGE CLASS	F	Static
Plug valve	KURVALF	RF-VP	F	Static
Needle valve	DANILO	50PM14025	SW	Static
Ball valve	NUOVAFIMA	BSV/VV	SW	Static
Pilot-operated pressure regulator	FIORENTINI	REFLUX-819 P.207/A+R14 SB-105	F	Dynamic
Cartridge Filter	FIORENTINI	HFA/1	F	Dynamic
Turbine flow meter	ELSTER	TRZ2 G100 A1R/A 1S	F	Dynamic

*F stands for flanged coupling and SW stands for screwed coupling

As depicted in Figure 1, the static section consists in several lines in which three testing valves can be installed. Each line is equipped with a pressure transmitter and an analysis port to monitor the pressure level and the gas quality in the line during the test, and two sectioning valves (see Figure S2). The lines were fed with the 20 mol % H_2 blend at 80 barg and the sectioning valves closed, isolating each line. The lines stayed this way for the 3000 h that the test lasted. During the test, the pressure was monitored, and the admixture composition checked periodically using a gas analyzer (NOVA 5300SPK).

5

2.3. Hydrogen sensitivity tests

Possible hydrogen embrittlement on pipes and further damage on components or equipment of the high-pressure natural gas grid due to the presence of hydrogen was studied in the dynamic section of the testing platform. The testing elements were installed in a piping system that forms a closed loop working at 80 barg, where a constant flow of gas is achieved thanks to the combined operation of a gas compressor (8AGD-5 booster, Haskel) and a pressure regulator (Reflux, Fiorentini) downstream (see Figure 1). As testing equipment, a filter, pressure regulator and gas meter have been installed, trying to reproduce a pressure regulation station of the transmission grid. The characteristics of this equipment are also explained in Table 1. The equipment was working at 80 barg for 3000 h exposed to the 20 mol % H_2 blend. At the end of the test, all the items were disassembled and their different parts (springs, membranes, O-rings, etc.) inspected with the aid of a stereo microscope with a camera, to detect cracking or other type of hydrogen damage, such as blistering.

As testing pipes, steels of different API 5L qualities (grade X42, X52, X60 and X70) have been selected. These steels were found to be the most representative in European transmission grid in our previous research.[23] The as received chemical composition, mechanical properties and microstructure of the base and welded API5L steels were determined (see Figure 2). A relation of the main properties of API5L steel pipes under study can be found in the Supporting Information (see Table S1).
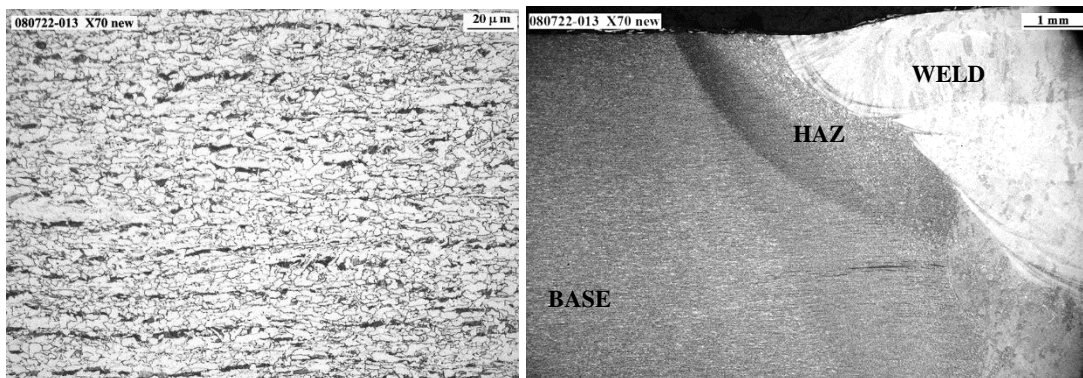

Figure 2. Optical micrographs showing detail of the ferrite (white)+ bainite (black) microstructure in X70 steel (left) and cross section of GTA welded joint in X70 steel (right)

The tests on steels have been performed as normalized constant displacement (constant strain) specimens that were mechanized from base and welded X42, X52 and X60 OD 6" pipes and from base and welded X70 OD 16" pipes (see Figure S3). An important benefit of using static loaded specimens is that once the deformation has been applied to the specimen, the self-loading assemblies may be inserted into loops or closed test vessels and exposed to the hydrogen environment at a certain pressure. A pig trap has been installed in the dynamic section of the testing platform, aiming as autoclave that can operate at 80 barg and in which the strain specimens have been allocated for the test. Three types of constant displacement specimens have been developed in this work: C-ring, four-point bend (4pb) and pre-cracked compact tension (CT) wedge opening load (WOL) specimens, which have been exposed to the 20 mol % H_2 blend at 80 barg for 3000 h inside the pig trap (see Figure 3).
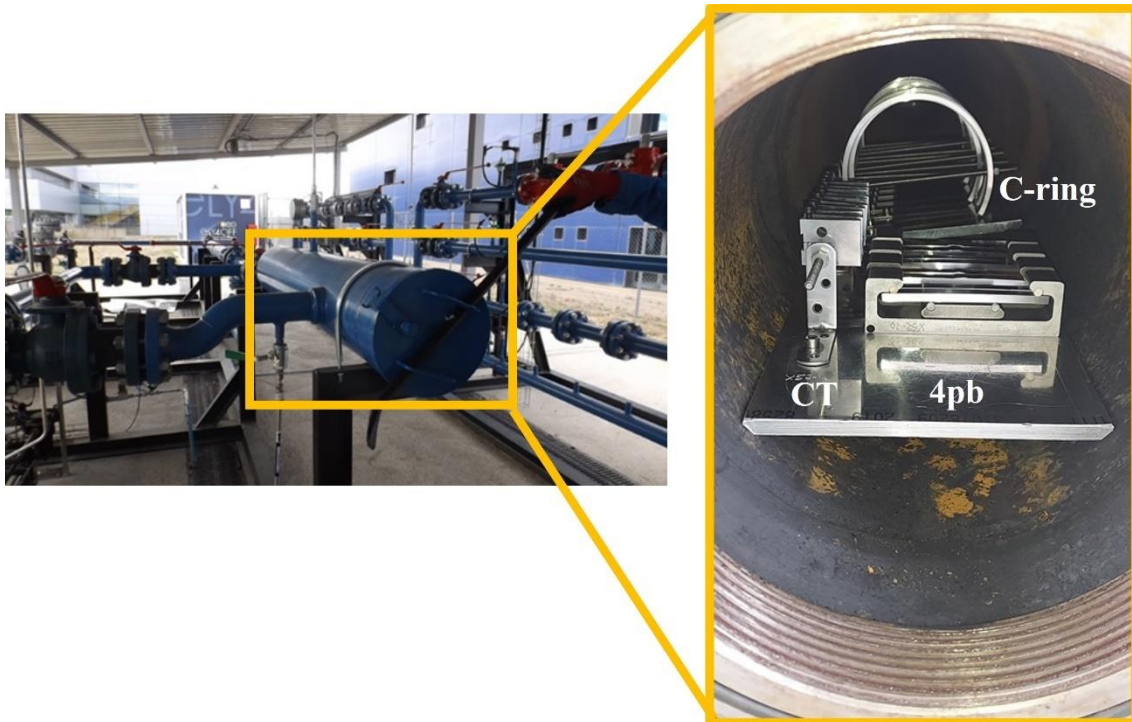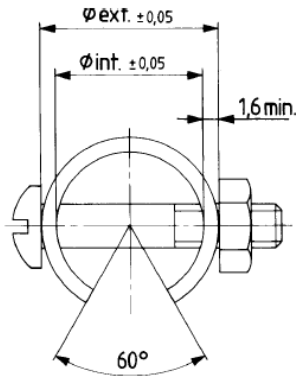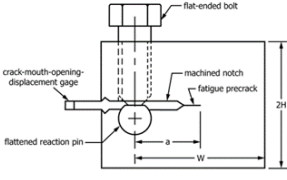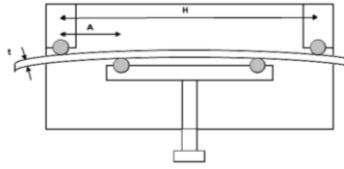
6

Figure 3 Picture of the strained specimens allocated inside the pig trap for the test.

C-rings specimens are made from tubular products and are bolt loaded to the desired stress level, usually reported as a percentage of the yield strength. Deflections should be limited to stresses comprised between 75 and 100 % of the elastic limit. Due to the circumferential welding of the pipe sections, C-ring specimens have been machined out only from the base metal. The 4pb specimen is subjected to a constant tension that is performed by supporting the beam specimen on two loading rollers and applying a load through two other rollers. Deflections should be limited to stresses usually comprised between 75 and 100 % of the elastic limit. 4pb base and welded specimens have been tested. The welded specimens were taken transverse to the circumferential weld, with the weld bead at the center of the specimen. The evaluation of the material resistance to the environment was realized by examining the tested C-ring and 4pb specimens by optical and scanning electron microscopy (SEM) for evidence of cracking. The CT-WOL fatigue pre-cracked specimen can be self-loaded by tightening a bolt against a taper pin, to produce a constant displacement at the loading points. The stress intensity factor applied to the WOL specimen (K_{IAPP}) can be estimated according to ASTM E1681.[28] The loaded CT-WOL specimen was kept in the loaded condition during the hydrogen exposure tests. At the conclusion of the test, the CT specimens were examined by SEM to assess if subcritical cracking occurred from the initial fatigue crack. Measurements of the crack front extent were taken in three positions and the average crack growth in hydrogen was calculated. According to ASTM E1681 standard,[28] there is no fatigue pre-crack growth if the average measured crack growth does not exceed 0.25 mm. Details of the three normalized constant displacement specimen types are given in Table 2 and the specific procedure on their preparation process can be found in the Supporting Information.

Table 2. Types of constant displacement specimens used in the testing platform and summary conditions.

	Constant displacement specimens		
Type of specimen	**C-ring**	**CT-WOL**	**4pb**
Condition of specimen	Smooth / notched	Notched pre-cracked	Smooth
Base/weld material	Base	Base and weld joint	Base and HAZ
Standards	ISO 7539-5,[25] ASTM G38[26]	ISO 7539-6,[27] ASTM E1681[28]	ISO 7539-2,[29] ASTM G39[30]
Yield strength (%)	100 % YS	-	100 % YS
Specimen geometry and size (in mm)	d = Tube OD t = tube thickness w = 20	t = greatest thickness allowed by the bent and thickness of the pipe (at least 85% of the pipe thickness)	H = 100 w=10 t = thickness=5-6
Steel grades	X42, X52, X60, X70	X52, X70	X52, X70
Number of specimens	1 for each steel grade	3 base, 2 welded joints for each steel grade	2 base, 2 welded joints for each steel grade
Environment	20 mol % H_2 in CH_4		
Test duration	3000 h		
Post testing evaluation	Evidence of cracking in C-ring and 4-pb specimens. Inspect for crack growth in CT-WOL specimen. Metallographic/fractographic examination by optical and SEM microscopy		

2.4. Gas separation test

The separation of hydrogen from methane has also been considered in this work, thinking in potential customers that demand natural gas with high quality and want to remain connected to the grid when the fuel comes blended with hydrogen (e.g. industries that use natural gas as feedstock to produce methanol and ammonia). Hydrogen recovery is necessary in these cases, so that the natural gas can be "purified" prior its consumption.

A gas separation prototype based on membrane technology has been developed in the experimental testing facility to perform H_2/CH_4 gas separation tests, where the long-term permeation properties of the prepared membranes has been studied. Pd-based double-skinned membranes deposited onto 14 mm OD porous ceramic tubes have been prepared

and integrated in the membrane prototype for this study, following the preparation procedure reported by Arratibel et. al.[31]. The first campaign was carried out by using Membrane #1 with 22.1 cm long and the second testing campaign by using Membrane #2 of 21.7 cm long. Pd-based membranes have been selected because of their high hydrogen permeance and selectivity compared to other materials. The gas separation prototype consists in three parts: the feed section, the membrane reactor and an analysis section (see Figure S4). At the feed section, a mass flow controller (Bronkhorst) set the desired feed flow rate. The feed section is connected to the blending station of the experimental platform that generates the H_2/CH_4 blend for the test. The Pd-based tubular membranes were placed inside the reactor. It is composed of a feeding line, coming from the feed section, and two outlets (permeate and retentate). The permeate is the stream rich in hydrogen, and the retentate, that rich in methane. The heating of the reactor was performed by the tubular furnace with an internal diameter of 110 mm and an active length of 600 mm. The oven has three heating zones which allows optimal control of the whole active zone length. A back-pressure regulator (Bronkhorst) is placed at the outlet of the retentate side to set the required trans-membrane pressure difference. The retentate and the permeate lines are connected to the analysis section. It contains mass flow meters (Bronkhorst) to measure and monitor the permeate and retentate flows. The outlet gases from both retentate and permeate sides can be analyzed with the NOVA 5300SPK gas analyzer.

Two different Pd-based membranes have been tested in the prototype. In a first experiment the long-term stability of this kind of membranes was tested under a constant feed flow (8.3 $Nl·min^{-1}$) and feed pressure (80 barg). In a second round of tests, the feed pressure was varied (10, 20, 40, 60, 80 barg) and then feed flow was tuned for obtaining the maximum H_2 recovery for each feed pressure.

With Membrane #1, mixed gas tests were performed at 400 °C feeding 8.33 $Nl·min^{-1}$ of the H_2/CH_4 blend (20 mol % H_2) at 80 barg to the membrane module. The mixed gas test consisted in 5 cycles of 100 h each, maintaining the system at operating pressure but without feed flow between cycles. The permeate flow and hydrogen content in the permeate stream were monitored to assess the gas separation performance of the membranes.

With Membrane #2 feed flow and pressure were modified between 1.12-6.15 $Nl·min^{-1}$ and 10-80 barg for the mixed gas tests, respectively, maintaining the operating temperature always at 400 °C. The permeate flow and hydrogen concentration in the permeate stream were monitored to calculate the hydrogen recovery. The whole experiment lasted 175 h.

3 RESULTS AND DISCUSSION

3.1 Tightness of testing valves to the blend

The tightness of some of the most representative kind of valves that can be found in the transmission grid has been tested, operating them at 80 barg with a H_2/CH_4 blend with 20 mol % hydrogen content. The evolution of the pressure and the composition of the gas (mol % H_2) for each line of the static section during the time of the experiment is given in Figure 4. A pressure drop would mean a critical tightness failure, while the loss of hydrogen owing to preferential permeance over methane would be identified by a

9

decrease in the hydrogen concentration in the blend. The reference line contains no testing element and serves as blank test. There are also two lines that include only flanged or screwed couplings, respectively. These lines also serve as reference tests because they help to distinguish whether a possible leakage comes from the coupling or the body of the valve.

Figure 4 shows how there are no critical pressure losses in any branch of the system, and the pressure oscillations (76.7 ± 4.5 bar, as the widest interval for the line with ball valves with flanged couplings) correspond to temperature changes from day to day, as well as between night and day. The gas composition remains basically constant in all the reference lines, being the oscillation shown within the measuring error of the analyzer (<1 mol %) and in all cases below 0.5 mol %. This means that neither the line itself nor the couplings (flanged or screwed) add significant hydrogen losses in the system and can be considered tight. The same behavior can be observed for the different lines containing test valves, except for those containing ball and needle valves with screwed couplings. Since the line containing just screwed couplings does not show a noticeable hydrogen loss, the losses observed in these other branches must occur through the body of the valves. Based on the dimensions of the line (volume of 17.2 L), the total average leakage rate of hydrogen in both lines was 2.9 $Nml \cdot h^{-1}$, leading to less than 1 $Nml \cdot h^{-1}$per valve if the same rate in each item is considered. These losses are negligible and cannot be considered critical. In any event, they can be solved by installing a screwed cap at the other side of the valves or connecting a device, such as a manometer. It is strange to find them unconnected in gas pipelines, except for venting lines. All the valves tested can be therefore considered ready for operation under the hydrogen blend studied because the leakages found were minimal.
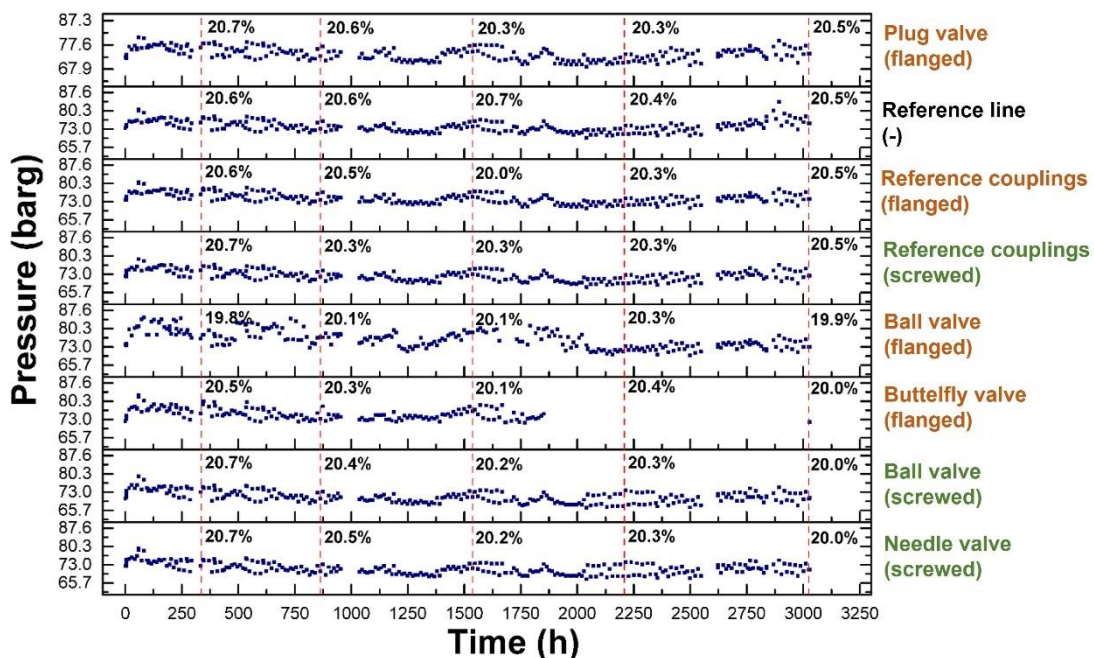

Figure 4. Evolution of the pressure (blue scatter) and gas composition (mol % H_2) in each line of the static section during the experimental campaign.

3.2 Hydrogen sensitivity of steels, components and equipment

All the test specimens (C-ring, 4pb and CT-WOL specimens) were placed inside the pig trap in the loop experimental platform and exposed for 3070 hours to a gas atmosphere composed of a 20 mol % H_2 blend in CH_4. The gas pressure was established at 80 barg and dynamic flow conditions (60 $m^3N·h^{-1}$) were applied. At the end of the test, the pig trap was purged with nitrogen and opened. At the time of opening, no corrosion was observed on the steel samples. However, once the outside air entered the pig trap, and due to the existing humidity, a slight corrosion was produced on the surface of the steel specimens.
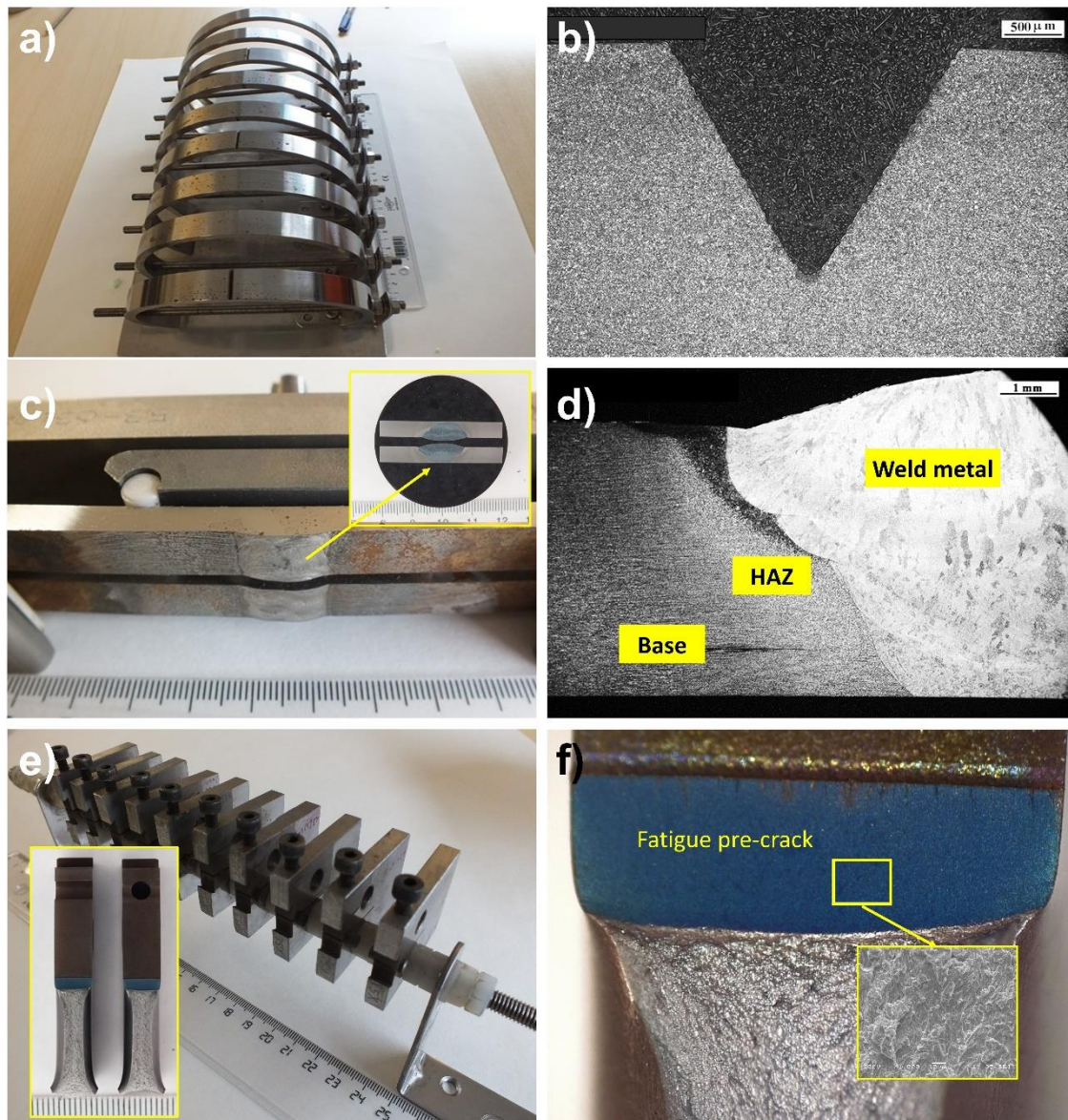
Figure 5. a) Detail of the tested C-ring specimens, b) optical micrograph of notched C-ring section from steel grade X60 with metallographic etching, c) detail of 4pb X70 welded steel specimens and metallographic probe (inset), d) optical micrograph of welded cross section from steel grade X70 (with metallographic etching), e) detail of rack with tested CT-WOL specimens and detail of the two fracture surfaces (inset) and f) detail of the "tinted" fatigue precrack fracture surface with SEM micrograph as inset.

Figure 5a shows the appearance of the C-ring specimens after their removal from the pig trap. No cracks were detected after optical inspection with a LEICA S9i stereo microscope. Optical and SEM (JEOL 5910-LV) microscope examination of metallographic cross sections confirms the absence of cracks in notched samples (see

11

Figure 5b). Figure 5c shows the appearance of tested welded X70 4pb specimens supported in the loading jig. No cracks were detected during the inspection with the stereo microscope. Metallographic sectioning in Figure 5d also confirms the absence of cracks in the welded joint specimens. Figure 5e shows the appearance of the rack with the tested CT-WOL specimens after being removed from the pig trap. The CT specimens were unloaded (removing the bolt) and then heat tinted (30 min at 300 ºC) and broken to evaluate if the initial fatigue pre-crack (generated in air before exposing the specimen to the hydrogen blend) had grown (see Figure 5f). The fracture surface was examined by optical and SEM microscopy and measurements of the crack front extent were carried out. No hydrogen crack growth was noticed for any CT-WOL specimen and thus the crack propagation was <0.25mm. The results for the CT specimens testing are summarized in Table 3.

Table 3. Results of CT-WOL specimens testing.

Gas atmosphere	Steel grade (number of specimens)	Test duration (h)	Notch position / crack plane orientation	Crack propagation after exposition	Applied initial stress intensity (K_{IAPP}) in $MPam^{1/2}$
20%H_2/80%CH_4 80 barg	X52 (3)	3070	Base / TL	<0.25mm	32
	X52 HAZ (2)		HAZ / TL	<0.25mm	32
	X70 (3)		Base / TL	<0.25mm	41
	X70 HAZ (2)		HAZ / TL	<0.25mm	41

Besides the analysis of the four API steel grades, this work has also considered the inspection and analysis of other components and equipment of the high-pressure natural gas grid. The main body of the plug, ball and butterfly valves (flanged coupling), present in the static section of the experimental platform, have been disassembled at the end of the test and inspected to detect signs of hydrogen damage. The main parts of the filter and pressure regulator have also been characterized following the same methodology. After visual inspection with a stereo microscope with camera, some slightly damaged areas, mainly owing to linear or scratch abrasion in certain components, could be observed. Apart from this, no clear signs of hydrogen damage were observed on the different parts inspected. (Figures S5 to S14) show the general appearance and some more detailed analysis of some of the examined items.

3.3 Gas separation performance of the membrane prototype

The deblending of the 20/80 (mol %) H_2/CH_4 admixture was tackled with a gas separation prototype containing double-skinned Pd-based membranes. Long-term stability tests under constant feed flow and pressure as well as test under variable feed condition were performed in this prototype with two different membranes.

3.3.1 Long-term stability test under constant feed flow and feed pressure

The long-term stability of Membrane #1 towards the separation of 20/80 (mol %) H_2/CH_4 blends at 80 bar feed pressure was tested in a first approach. The gas separation performance of this first membrane for 500h operation is shown in Figure 6.
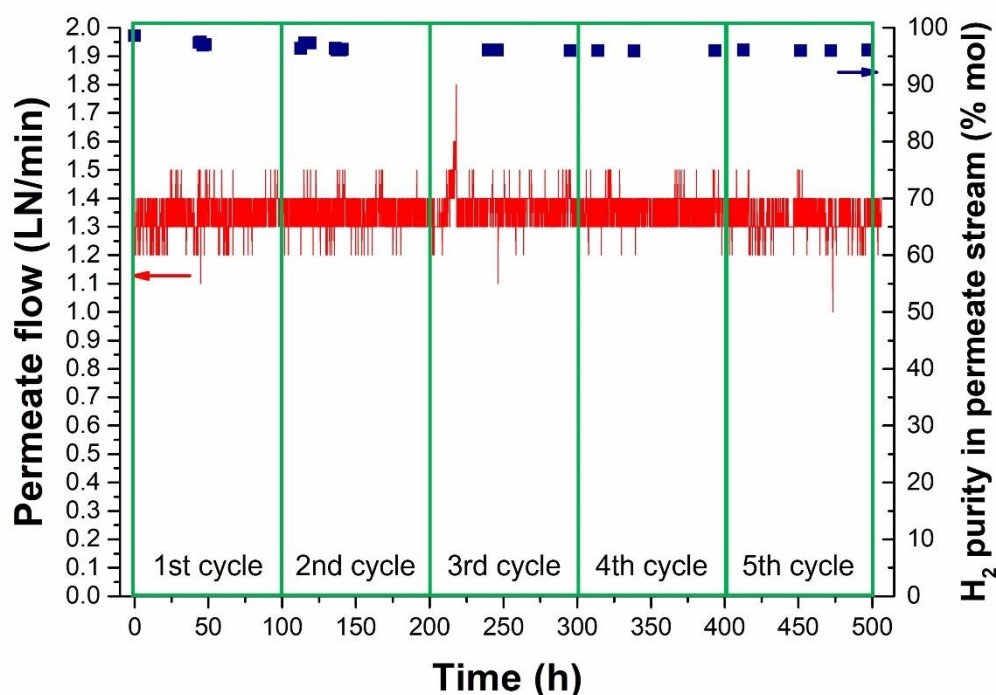
Figure 6. Gas separation performance of the membrane prototype with Membrane #1 for the tests under constant feed flow and feed pressure. Red line stands for the total permeate Flow and blue scatter stands for the H_2 purity in the permeate stream.

The permeate flow (that rich in hydrogen obtained at atmospheric pressure) has been quantified during the test and its composition analyzed periodically in the different cycles comprising the test. It can be seen how the permeate stream remains mainly constant during the whole operation, with a mean value of 1.35 ± 0.06 Nl·min^{-1}. The hydrogen purity in the permeate stream begins being of 98.6 mol % and decreases slightly from the second cycle on. In any event, its values are always above 96.0 mol % H_2. Since both the feed and the permeate flows are completely defined, the retentate stream can be calculated with a mass balance (see Supporting Information). This calculation leads to a retentate flow of 6.93 – 7.03 Nl/min with a hydrogen content between 3.5 and 5.7 mol %. The CH_4 purity of the retentate stream (in this case, 94.3-96.5 mol%) may be sufficient for end-users demanding a high natural gas quality. If required, the CH_4 content in the retentate could be increased by e.g. increasing the membrane area.

3.3.2 Tests under variable feed flow and feed pressure

Gas separation tests were also performed with Membrane #2. Firstly, the feed flow was maintained at 8.3 Nl/min and feed pressure was varied (Table 4 – top). Then, the feed flow was modified for each feed pressure during the test to tune the permeate stream towards obtaining the maximum hydrogen recovery possible (Table 4 – bottom).

The permeate flow (rich in hydrogen) was monitored and its composition analyzed periodically during the different cycles of the test. The obtained results about H_2 content in the retentate and permeate streams and hydrogen recovery are summarized in Table 4. The decrease of the feed flow maintaining the feed pressure increases the hydrogen flow in the permeate subsequently increasing the hydrogen recovery rate and reducing the

hydrogen content in the retentate stream. The hydrogen purity in the permeate stream was higher than 99.5 mol% after the 175 h of the testing campaign and, therefore, a hydrogen concentration value down to 2.7 mol% is achieved in the retentate stream when tuning the operating conditions. This is the highest hydrogen recovery value obtained (i.e. 90.0 mol%).

Table 4. Gas separation performance of the Membrane #2 for the tests under: (top part) same feed low and variable feed pressure; (bottom part) variable feed flow and feed pressure with the aim at maximizing the hydrogen recovery factor.

Total feed flow ($Nl \cdot min^{-1}$)	Feed pressure (barg)	mol% H_2 permeate	mol% H_2 retentate	%H_2 recovery
8.30	10	99.9	14.9	30.1
8.30	20	99.8	10.3	54.1
8.30	40	99.6	7.8	66.0
8.30	60	99.5	6.6	71.9
8.30	80	99.5	5.3	77.9
Total feed flow ($Nl \cdot min^{-1}$)	Feed pressure (barg)	mol% H_2 permeate	mol% H_2 retentate	%H_2 recovery
1.12	10	99.8	12.2	44.6
2.24	20	99.8	7.6	66.9
3.12	40	99.6	4.8	79.9
4.63	60	99.5	3.4	85.9
6.15	80	99.5	2.7	90.0

4 CONCLUSIONS

The suitability of the main carbon steels (API 5L Gr X42, X52, X60 and X70), valves (ball, plug, butterfly and needle types), fittings (flanged and screw couplings) and equipment (filters, pressure regulators and gas meters) present in European high-pressure gas grids for the transport of 20 mol % H_2 blends in CH_4 at 80 barg has been tested under relevant environment at pilot scale. The experimental platform consists of a blending station that prepares and delivers the admixture at high pressure to the testing facilities. The testing platform itself includes a static section to perform tightness tests, a dynamic section to assess possible damage owing to hydrogen exposure and a gas separation prototype to achieve the H_2/CH_4 blend separation.

Most of the valves tested remained tight over 3000 h, with just minor hydrogen losses via the permeation mechanism through the body of screwed ball and needle valves. After disassembling the valves, a careful visual inspection showed no apparent damage on the different parts. An equivalent methodology led to the same conclusion with the cartridge of the filtering unit and the main parts of the pressure regulator. After more than 3000 h exposure to the hydrogen blend at 80 barg, the strained C-Ring and 4pb specimens showed no cracking in the inspection of the surface and metallographic cross-section

14

examinations. Neither the base material, nor the HAZ, nor the welded material showed any signs of embrittlement or other kind of damage. No subcritical crack propagation under constant displacement could neither be noticed in CT-WOL specimens. Therefore, based on the tested conditions, the different pipes, components and equipment considered in this work may be suitable for the transport of hydrogen blends with hydrogen content up to 20 mol % at ≤ 80 barg. Nevertheless, further research is necessary to assess possible negative effects of impurities in the blend. The tolerance to other blends with higher content of hydrogen is another fact that needs to be enlightened.

Hydrogen and methane separation from the blended 20 mol % H_2 at 80 barg was also investigated. The hydrogen and methane separation capability of a gas separation prototype containing Pd-based double-skinned membranes was used for this task. The long-term stability experiment of Membrane #1 led to a good gas separation performance, where the prototype showed a stable permeate flow during the 500h operation with a hydrogen purity over 96%. In the case of Membrane #2, feed flow and feed pressure were tuned to obtain the maximum hydrogen recovery possible, reaching 90% at 80 barg feed pressure and 6.15 $Nl \cdot min^{-1}$ feed flow with the lowest H_2 content in the retentate of 2.7 mol%, and H_2 purities in the permeate higher than 99.5 mol% after 175 h operation. These results show that the membrane technology is promising for the H_2 recovery and purification of low H_2-concentrated gas streams.

ACKNOWLEDGEMENTS

BIBLIOGRAPHY

1. Armaroli, N. and V. Balzani, *The Hydrogen Issue.* ChemSusChem, 2011. **4**(1): p. 21-36.
2. Almansoori, A. and A. Betancourt-Torcat, *Design of optimization model for a hydrogen supply chain under emission constraints-A case study of Germany.* Energy, 2016. **111**: p. 414-429.
3. Lehner, M., et al., *Power-to-gas: technology and business models*. 2014: Springer.
4. Chapman, A., et al., *A review of four case studies assessing the potential for hydrogen penetration of the future energy system.* International journal of hydrogen energy, 2019. **44**(13): p. 6371-6382.
5. Haeseldonckx, D. and W. D'haeseleer, *The use of the natural-gas pipeline infrastructure for hydrogen transport in a changing market structure.* International Journal of Hydrogen Energy, 2007. **32**(10-11): p. 1381-1386.
6. (ENTSOG), E.N.o.T.S.O.f.G., *DECARBONISING THE GAS VALUE CHAIN. CHALLENGES, SOLUTIONS AND RECOMMENDATIONS* 2021.
7. Tabkhi, F., et al., *A mathematical framework for modelling and evaluating natural gas pipeline networks under hydrogen injection.* International journal of hydrogen energy, 2008. **33**(21): p. 6222-6231.

8.   Amber Grid, B., Conexus, CREOS, DESFA, Elering, Enagás, Energinet, Eustream, FGSZ, FluxSwiss, Fluxys Belgium, Gas Connect Austria, Gasgrid Finland, Gassco, Gasunie, Gas Networks Ireland, GAZ-SYSTEM, GRTgaz, National Grid, NET4GAS, Nordion Energi, OGE, ONTRAS, Plinacro, Plinovodi, REN, Snam, TAG, Teréga, and Transgaz, *Hydrogen European Backbone*. 2022.

9.   Park, C., C. Kim, and Y. Choi, *Power output characteristics of hydrogen-natural gas blend fuel engine at different compression ratios.* International journal of hydrogen energy, 2012. **37**(10): p. 8681-8687.

10.   Wang, J., et al., *Study of cycle-by-cycle variations of a spark ignition engine fueled with natural gas–hydrogen blends.* International journal of hydrogen energy, 2008. **33**(18): p. 4876-4883.

11.   Xu, J., et al., *Experimental study of a single-cylinder engine fueled with natural gas–hydrogen mixtures.* International journal of hydrogen energy, 2010. **35**(7): p. 2909-2914.

12.   Dwivedi, S.K. and M. Vishwakarma, *Hydrogen embrittlement in different materials: A review.* International Journal of Hydrogen Energy, 2018. **43**(46): p. 21603-21616.

13.   San Marchi, C.W. and B.P. Somerday, *Technical reference for hydrogen compatibility of materials*. 2012, Sandia National Laboratories (SNL), Albuquerque, NM, and Livermore, CA ….

14.   Ronevich, J.A., et al., *Hydrogen-assisted fracture resistance of pipeline welds in gaseous hydrogen.* International Journal of Hydrogen Energy, 2021. **46**(10): p. 7601-7614.

15.   San Marchi, C., et al. *Fracture and fatigue of commercial grade API pipeline steels in gaseous hydrogen*. in *Pressure Vessels and Piping Conference*. 2010.

16.   Stalheim, D., et al. *Microstructure and mechanical property performance of commercial grade API pipeline steels in high pressure gaseous hydrogen*. in *International Pipeline Conference*. 2010.

17.   Capelle, J., et al., *Sensitivity of pipelines with steel API X52 to hydrogen embrittlement.* International Journal of Hydrogen Energy, 2008. **33**(24): p. 7630-7641.

18.   Briottet, L., I. Moro, and P. Lemoine, *Quantifying the hydrogen embrittlement of pipeline steels for safety considerations.* International journal of hydrogen energy, 2012. **37**(22): p. 17616-17623.

19.   Slifka, A.J., et al., *Fatigue measurement of pipeline steels for the application of transporting gaseous hydrogen.* Journal of Pressure Vessel Technology, 2018. **140**(1).

20.   Pluvinage, G., *Mechanical properties of a wide range of pipe steels under influence of pure hydrogen or hydrogen blended with natural gas.* International Journal of Pressure Vessels and Piping, 2021. **190**: p. 104293.

21.   Shao, L., et al., *Polymeric membranes for the hydrogen economy: contemporary approaches and prospects for the future.* Journal of Membrane Science, 2009. **327**(1): p. 18-31.

22.   Bakhtiari, O., et al., *Preparation, characterization and gas permeation of polyimide mixed matrix membranes.* J. Membr. Sci. Technol, 2011. **1**(1): p. 1-6.

23.   Michael Walter, A.B., Javier Sánchez-Laínez , Hiltrud, A.C.A. Schülken , Vanesa Gil, María Dolores, and S.d.G. Calvo, *D2.3 Final document review on specific technical, RCS barriers, enablers and innovations*. 2021.

24.   ISO, *Corrosion of metals and alloys. Stress corrosion testing. Part 6: Preparation and use of precracked specimens for tests under constant load or constant displacement. ISO 7539-6:2018.* 2018.

25.   *ISO 7539-5. Corrosion of metals and alloys – Stress corrosion testing – Part 5: preparation and use of C-ring specimens. No. 1, 1989.*

26.   *ASTM G38, Standard practice for making and using C-Ring stress-corrosion test specimens. ASTM G38-01(2021).*

27.   *ISO 7539-6, Corrosion of metals and alloys. Stress corrosion testing. Part 6: Preparation and use of precracked specimens for tests under constant load or constant displacement. ISO 7539-6(2018).*

28.   *ASTM E1681, Standard test method for determining threshold stress intensity factor for environment-assisted cracking of metallic materials. ASTM E1681-03(2008).*

29.   *ISO 7539-2, Corrosion of metals and alloys. Stress corrosion testing. Part 2: Preparation and use of bent-beam specimens. ISO 7539-2 (1989).*

30.   *ASTM G39, Standard practice for preparation and use of bent-beam stress-corrosion test specimens. ASTM G39-99(2021).*

31.   Arratibel, A., et al., *Development of Pd-based double-skinned membranes for hydrogen production in fluidized bed membrane reactors.* Journal of Membrane Science, 2018. **550**: p. 536-544.

SUPPORTING INFORMATION

Table of contents of the Supporting Information
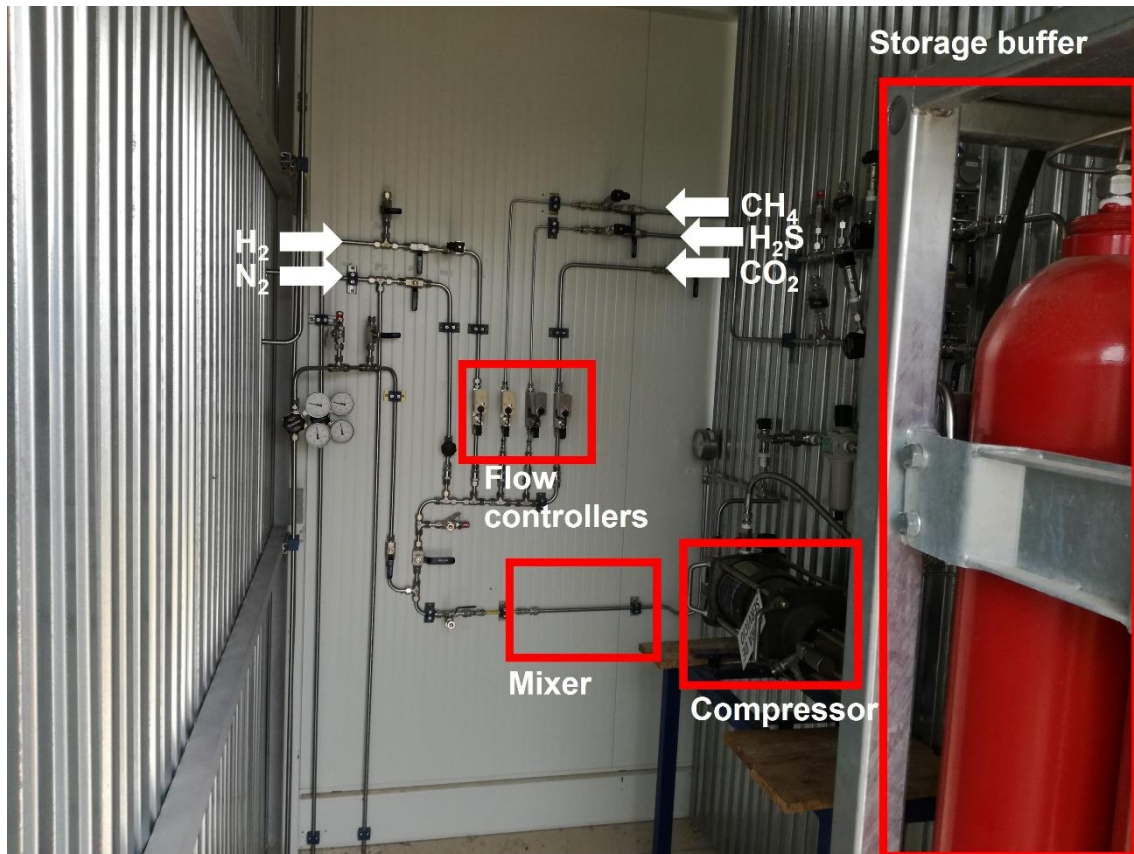
Sections of the R&D platform

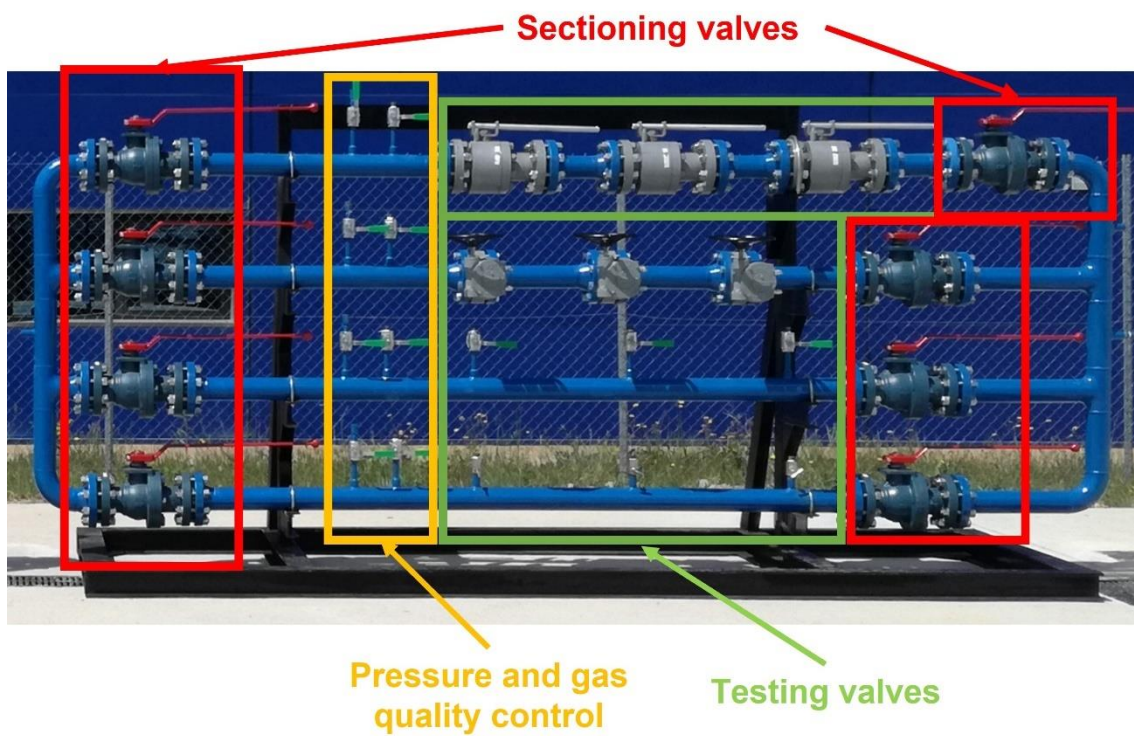*Figure S1. Picture of the blending station of HIGGS' R&D platform*

Figure S2. Picture of part of the static section of the testing platform where tightness tests are performed

Preparation of constant displacement specimens

Figure S3. Photographs showing detail of the two sections of the X70 steel pipe as example

Table S1 Summary of properties of the API5L steel pipes under study

API 5L steel grade	Nominal diameter (in)	Outside diameter (in)	Wall thickness (mm)[1]	Yield strength (Mpa)		Ultimate tensile strength (Mpa)		Welding procedure /filler material	Microstructure (base steel)
				Tensile testing (ISO 6892)[2]	API 5L (min.)	Tensile testing (ISO 6892)	API 5L (min.)		
X42	6	6.625	6.9	451	290	542	415	GTAW[3]/ER70S-6	Ferrite + perlite
X52	6	6.625	7.8	440	360	514	460	GTAW/ER70S-6	Ferrite + perlite
X60	6	6.625	7.8	510	415	581	520	GTAW/ER90S-B3	Bainite
X70	16	16.00	8.2	549	485	675	570	GTAW/ER90S-B3	Ferrite + bainite

[1]Thickness obtained from metallographic cross sections

[2] Average value of two tensile tests

[3] Gas Tungsten Arc Welding (GTAW)

C-ring specimens

The design, machining, and process for stressing the C-ring specimens has been carried out according to standards ASTM G38: *Standard practice for making and using C-Ring stress-corrosion test specimens* and ISO 7539-5: *Corrosion of metals and alloys. Stress corrosion testing. Part 5: Preparation and use of C-ring specimens*. The C-ring, as generally used, is a constant-strain specimen with tensile stress produced on the exterior of the ring by tightening a bolt centered on the diameter of the ring. According both standards, the final outside diameter (OD) required to give the desired stress is calculated on the basis of the following equation:

$$OD_f = OD - \Delta$$
$$\Delta = f\pi D^2 / 4EtZ \qquad \text{eq.1}$$

where:

OD = outside diameter of C-ring before stressing (mm)

OD_f = outside diameter of stresses C-ring (mm)

f = desired stress (MPa). The stress applied corresponds to the 100% of the steel´s yield strenght

Δ = change of OD giving desired stress (mm)

D = mean diameter (OD-t) (mm)

t = wall thickness (mm)

E = modulus of elasticity (Mpa)

Z= a correction factor for curved beams

4pb specimens

The 4pb test is a constant displacement test that is performed by supporting a beam specimen on two loading rollers and applying a load through two other loading rollers, so that one face of the specimen is in tension and the other is in compression. 4pb specimens are flat strips of metal of uniform rectangular cross section and uniform thickness, except in the case of welded specimens. The design, machining, and process for loading the 4pb specimens has been carried out according to standards ISO 7539-2: *Corrosion of metals and alloys. Stress corrosion testing. Part 2: Preparation and use of bent-beam specimens* and ASTM G39: *Standard practice for preparation and use of bent-beam stress-corrosion test specimens*

The required deflection is measured at the center of the specimen in tension, using a dial gauge attached to the loading jig. The following equation has been used to set the deflection:

$$y = \frac{(3H^2 - 4A^2)\sigma}{12ET} \qquad \textbf{eq.2}$$

where:

σ = tensile stress. The stress applied corresponds to the 100% of the steel´s yield strenght

E = modulus of elasticity

t = specimen thickness

A = distance between the inner and outer supports

H = distance between the outer supports

CT-WOL specimens

The fatigue precracked CT-WOL specimen is loaded by a constant displacement method to a stress intensity K_{IAPP} value equal to a defined value. CT-WOL specimen geometry, fatigue precracking and bolt loading method are carried out using applicable rules of standards ISO 7539-6: *Corrosion of metals and alloys. Stress corrosion testing. Part 6: Preparation and use of precracked specimens for tests under constant load or constant displacement* and ASTM E1681: *Standard Test Method for Determining Threshold Stress Intensity Factor for Environment-Assisted Cracking of Metallic Materials*

The CT-WOL specimens used for the tests are limited in thickness by the geometry of the as received steel pipes X52 and X70. According to ASTM E1681 standard, the maximum load on the bolts, which is achieved for the maximum K_{IAPP} value under LEFM (linear

elastic fracture mechanics) conditions, can be obtained by means of the following equations.

- To guarantee plane strain conditions, the following restrictions shall be met:

$$B, a_0, W - a_0 \geq 2{,}5 \left(\frac{K_{IAPP}}{\sigma_{YS}}\right)^2 \quad \textbf{eq.3}$$

where:
a_0= original crack size
B= specimen thickness
W=specimen width
σ_{YS}=steel yield strenght

The maximum K_{IAPP} value for the thickness of the specimen under plane strain conditions has been obtained:

$$K_{IAPP}^{máx} \leq \sigma_{YS} \sqrt{\frac{B}{2{,}5}} \qquad \textbf{eq.4}$$

- To guarantee LEFM conditions, the uncracked ligament must meet the following condition:

$$W - a_0 \geq \frac{4}{\pi} \left(\frac{K_{IC}}{\sigma_{YS}}\right)^2 \qquad \textbf{eq.5}$$

In this case, the maximum K_{IC} value for the thickness of the specimen under LEFM conditions has been obtained:

$$K_{IC}^{máx} \leq \sigma_{YS} \sqrt{\frac{\pi(W - a_0)}{4}} \quad \textbf{eq.6}$$

Where K_{IC} is the critical linear-elastic plane-strain stress intensity factor

- The maximum load on the bolts (P), which is achieved for the maximum K_{IC} value under LEFM conditions, has been obtained by means of the following equations:

$$K \, IAPP = \left[\frac{P}{BW^{1/2}}\right] f\left(\frac{a_0}{W}\right) \rightarrow P_{máx} = \frac{B\sqrt{W}}{f\left(\frac{a_0}{W}\right)} K_{IC}^{máx} \quad \textbf{eq.7}$$

$$f\left(\frac{a_0}{W}\right) = \frac{\left(2 + \frac{a_0}{W}\right)}{\left(1 - \frac{a_0}{W}\right)^{\frac{3}{2}}} \left[0.886 + 4.64\left(\frac{a_0}{W}\right) - 13.32\left(\frac{a_0}{W}\right)^2 + 14.72\left(\frac{a_0}{W}\right)^3 - 5.6\left(\frac{a_0}{W}\right)^4\right] \quad \textbf{eq.8}$$

A value of $\frac{a_0}{W}$ of 0.3 has been considered.

The obtained values for K_{IAPP} and K_{IC} are given in Table S2.

Table S2 . Estimated maximum value of K$_{IAPP}$ and K$_{IC}$ for the HIGGS CT-WOL specimens

Steel grade	Thickness (mm)	K$_{IC}$ max. [MPa√m]	K$_{IAPP}$ max. [MPa√m]
X52	6.6	22.1	51.8
x70	7.0	28.1	65.9

Once the value of K$_{IAPP}$ to be applied is known, the CT-WOL specimen is fatigue precracked in air according to ASTM E1681 section 7.3.4. Fatigue crack lengths of approximately 2 mm are sought. Crack plane propagation is parallel to the longitudinal direction (TL). The force (P) to be applied is calculated from the selected K$_{IAPP}$ and the length of the pre-crack from equation 7.

Gas separation prototype
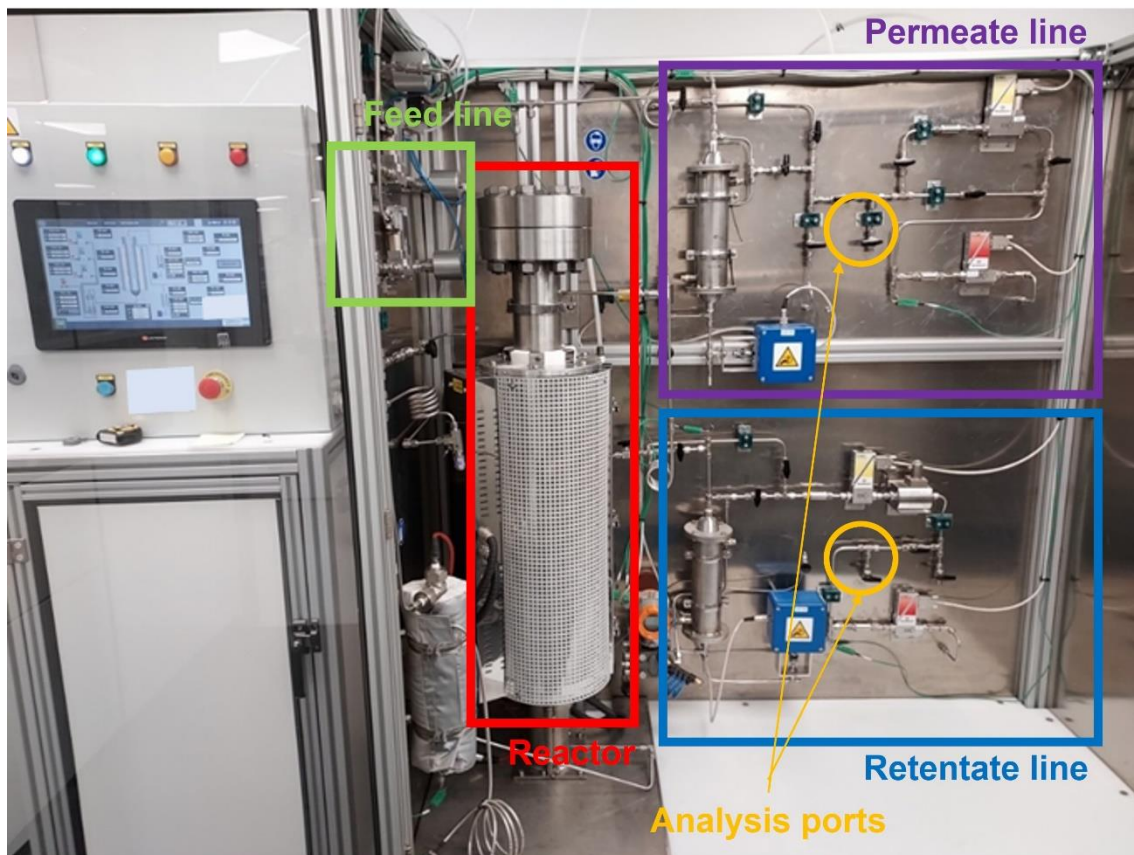
Figure S4. Picture of the gas separation prototype

Characterization of the main parts of the tested components and equipment

Main parts of the pilot operated pressure regulator
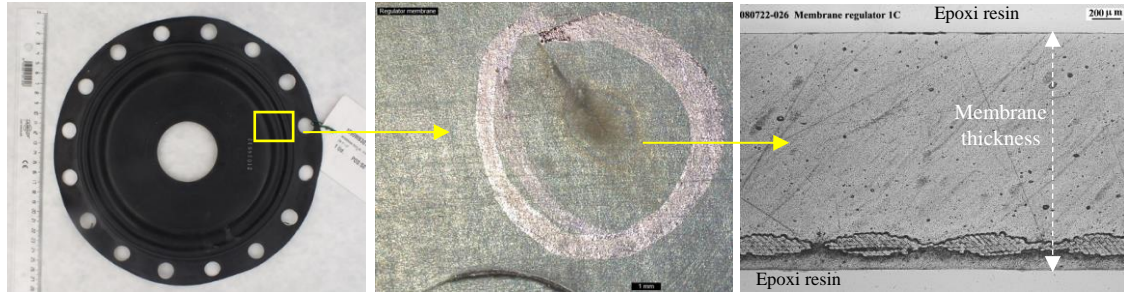
Figure S5. Parts of the presssure regulator: membrane: general appearance (left), detail of area with unknown damaged area (center) and cross section materialographic probe showing a very superficial damage
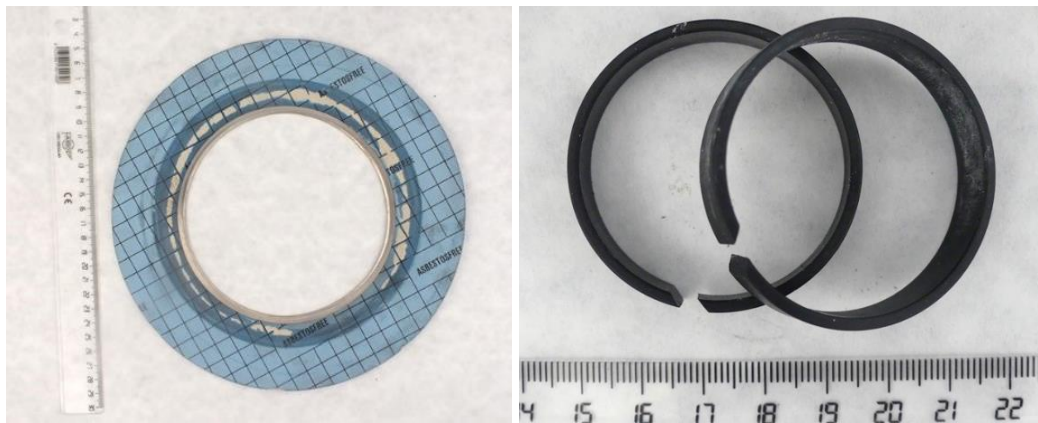

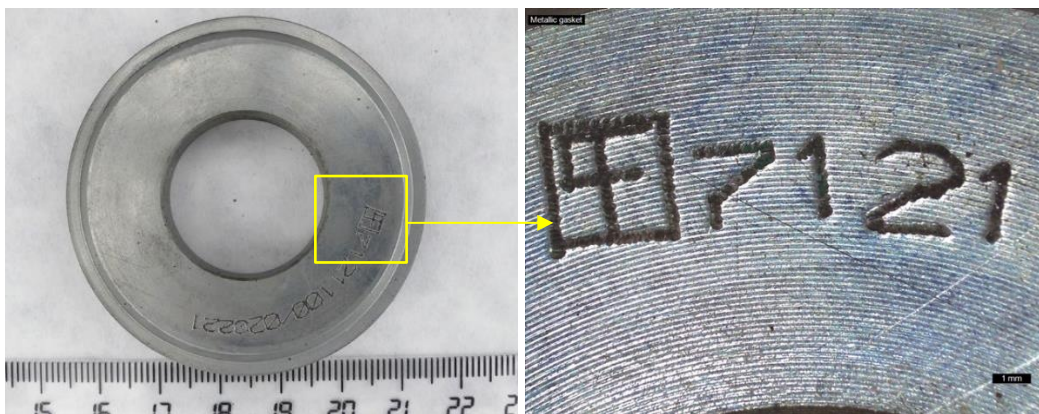*Figure S6. Parts of the pressure regulator: gasket (left) and guide rings (right)*

Figure S7. Parts of the pressure regulator: metallic gasket general appearance (left) and detail (right)
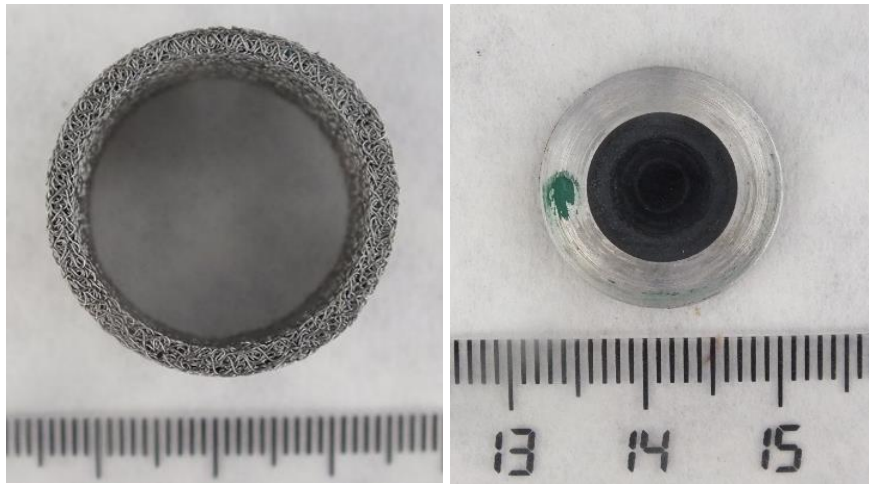
24

Figure S8. Prepilot: filter cartridge (left) and pad (right)

Figure S9. Prepilot: O-ring

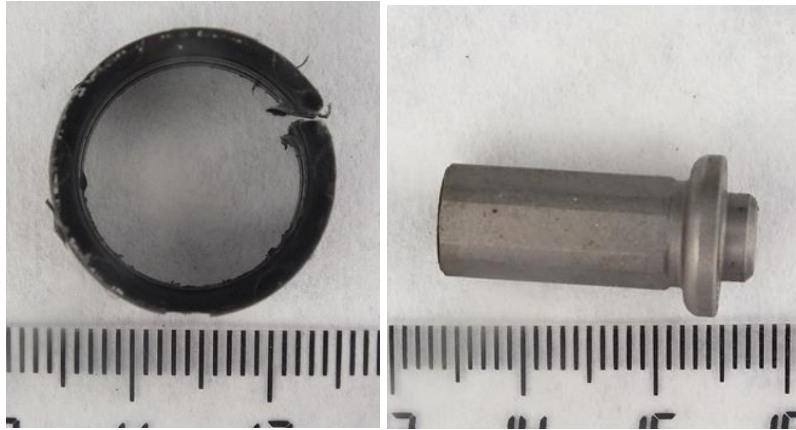*Figure S10. Pilot: membranes and guided rings (left) and detail of eroded area (right)*

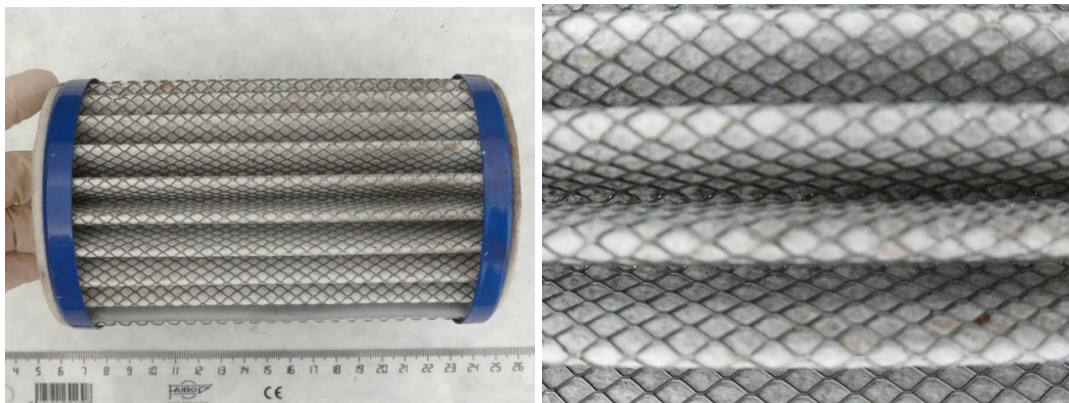*Figure S11. Pilot guide ring (left) and pilot metallic obturator (right)*

Figure S12. Filter cartridge

Main parts of the flanged testing valves

Figure S13. Spirometallic gaskets

Figure S14. Butterfly valve seal

Mass balance for calculating the retentate stream in the gas separation prototype

$$F = R + P$$

$$X_F \cdot F = X_R \cdot R + X_P \cdot P$$

where:

F=feed flow (8.3 Nl·min^{-1}=500 Nl·h^{-1})
R=retentate flow
P= permeate flow (1.35 Nl·min^{-1})
X_F=mol fraction of hydrogen in the feed stream (0.2)
X_R=mol fraction of hydrogen in the retentate stream
X_P=mol fraction of hydrogen in the permeate stream (0.986 or 0.960)